Atmos. Chem. Phys. Discuss., 12, 24243–24285, 2012
www.atmos-chem-phys-discuss.net/12/24243/2012/
doi:10.5194/acpd-12-24243-2012

Atmospheric Chemistry and Physics Discussions

Sulfate-nitrate-ammonium aerosols over China: response to 2000–2015 emission changes of sulfur dioxide, nitrogen oxides, and ammonia

Y. Wang[1], Q. Q. Zhang[1], K. He[2], Q. Zhang[1], and L. Chai[1]

[1]Ministry of Education Key Laboratory for Earth System Modeling, Center for Earth System Science, Institute for Global Change Studies, Tsinghua University, Beijing, China
[2]School of Environment, Tsinghua University, Beijing, 100084, China

Received: 6 August 2012 – Accepted: 27 August 2012 – Published: 17 September 2012

Correspondence to: Y. Wang (yxw@tsinghua.edu.cn)

Published by Copernicus Publications on behalf of the European Geosciences Union.

Abstract

We use a chemical transport model to examine the change of sulfate-nitrate-ammonium (SNA) aerosols over China due to anthropogenic emission changes of their precursors (SO_2, NO_x and NH_3) from 2000 to 2015. From 2000 to 2006, annual mean SNA concentrations increased by about 60 % over China as a result of the 60 % ~ 80 % increases in SO_2 and NO_x emissions. During this period, sulfate is the dominant component of SNA over South China (SC) and Sichuan Basin (SCB), while nitrate makes equal contribution as sulfate over North China (NC). Based on emission reduction targets in the 12th (2011–2015) Five Year Plan (FYP), China's total SO_2 and NO_x emissions are projected to change by −16 % and +16 % from 2006 to 2015, respectively. However, the amount of NH_3 emissions in 2015 is uncertain, given our finding that bottom-up inventories tend to overestimate China's ammonia emissions during the 2000–2006 period. With no change in NH_3 emissions, SNA mass concentrations in 2015 will decrease over SCB and SC compared to their levels in 2006, but increase over NC where the magnitude of nitrate increase exceeds that of sulfate reduction. This suggests that the SO_2 emission reduction target set by the 12th FYP, although effective in reducing SNA over SC and SCB, will not be successful over NC for which NO_x emission control needs to be strengthened. If NH_3 emissions are allowed to keep their recent growth rate and increase by +16 % from 2006 to 2015, the benefit of SO_2 reduction will be completely offset over all of China due to the significant increase of nitrate, demonstrating the critical role of NH_3 in regulating nitrate. The effective strategy to control SNA and hence $PM_{2.5}$ pollution over China should thus be based on improving understanding of current NH_3 emissions and putting more emphasis on controlling NH_3 emissions in the future.

ACPD
12, 24243–24285, 2012

1 Introduction

Sulfate, nitrate and ammonium (simplified as SNA) are the predominant inorganic species of fine particulate matter with diameters less than 2.5 µm ($PM_{2.5}$), making up approximately half of total $PM_{2.5}$ mass (Querol et al., 2004, Pinder and Adams, 2007; Tsimpidi and Karydis, 2007; Yang et al., 2011). SNA aerosols have adverse effects on human health, visibility degradation, and global climate change (Hillamo et al., 1998; Adams and Seinfeld, 1999; Watson, 2002; Park et al., 2004, 2006; Pathak et al., 2009; Leibensperger et al., 2012a, b). Most of SNA aerosols are formed in the atmosphere through oxidation and neutralization of precursor gases: sulfur dioxide (SO_2), nitrogen oxides ($NO_x = NO + NO_2$), and ammonia (NH_3). SO_2 is oxidized in the atmosphere by hydroxyl radicals (OH) in the gas phase, and by hydrogen peroxide (H_2O_2) and ozone (O_3) in the cloud. It is believed that the latter is the dominating approach of sulfate formation. Nitric acid (HNO_3) is formed through NO_x oxidized by OH and hydrolysis of N_2O_5. Sulfuric acid (H_2SO_4) and HNO_3 are neutralized by NH_3. $(NH_4)_2SO_4$ is the preferential species due to its stability. NH_4NO_3 is formed if excess NH_3 is available beyond the sulfate requirement. NH_4NO_3 is volatile and its formation is more significant in winter (Meng and Seinfeld, 1994; Ansari and Pandis, 1998; Seinfeld and Pandis, 1998; Adams and Seinfeld, 1999). SNA aerosols are water-soluble and subject to wet and dry deposition.

The concentrations and compositions of SNA aerosols are determined primarily by their precursors' emissions, which are mainly of anthropogenic origin. While SO_2 and NO_x emissions in the North Atlantic basin have been stabilized or are in decline, Asian emissions are still increasing (Benkovitz et al., 1996; Cofala et al., 2007; Smith et al., 2001, 2011). Emissions of SO_2 and NO_x in China increased dramatically by more than 60 % and 80 % respectively from 2000 to 2006 (Zhang et al., 2009; Lu et al., 2011). NO_x emissions in China were estimated to have maintained a mean annual growth rate of 6.7 % from 2006 to 2009 (Lamsal et al., 2011). Chinese SO_2 emissions were reported to have decreased by 9.2 % from 2006 to 2010 (Lu et al., 2011), driven primarily by wide

ACPD
12, 24243–24285, 2012

implementation of flue gas desulfurization in power plants. Agriculture is the largest contributor to NH_3 emissions. Bouwman et al. (1997) estimated that the global NH_3 emissions for 1990 were about 54 $Tg\,N\,yr^{-1}$ – about half of which were from Asia, with China accounting for the largest portion (Bouwman et al., 1997; Streets et al., 2003). In the 12th FYP (2011–2015), China set the emission reduction target for SO_2 and NO_x of 8 % and 10 %, respectively in 2015, compared to 2010 levels (http://www.gov.cn/zwgk/2011-09/07/content_1941731.htm). In light of the significant impact of SNA aerosols on public health and climate, it is important to understand the extent of SNA concentration changes in response to past and future changes of SO_2, NO_x and NH_3 emissions in China and to evaluate the effectiveness of currently-available emission control policies.

Previous studies have explored the response of SNA to precursor emission changes (Pinder and Adams, 2007; Tsimpidi and Karydis, 2007, 2008). They found that composite SNA levels did not respond linearly to SO_2 or NO_x emission changes with NH_3 playing an important role in determining total SNA concentrations. Most of the previous studies have focused on the US, where precursor emissions of SNA have been effectively controlled and $PM_{2.5}$ has been successfully incorporated into the national ambient air quality standard (NAAQS) and extensively monitored. China, despite facing serious $PM_{2.5}$ pollution problems, has not drawn up the corresponding control standard or monitoring network for SNA or $PM_{2.5}$. As a result, it is difficult to generate observation-based spatial distribution and temporal trend of SNA across China to guide the precursor control policies. It would require a credible chemical transport model, evaluated by scattered in-situ aerosol sampling in China; or satellite-derived proxies such as aerosol optical depth, to simulate the SNA distributions, associate their concentrations with precursor emissions, and predict the concentration changes in response to future emission changes.

In this study, we used a nested-grid version of a global chemical transport model (GEOS-Chem) to conduct full-year simulations of SNA over China. Model results are evaluated with a few surface observations in and around China. Our purpose is to understand the main factors determining the seasonal and spatial distributions of SNA

ACPD
12, 24243–24285, 2012

over China, investigate the influence of precursor emission changes on SNA concentration changes from 2000 to 2015, and provide policy suggestions for controlling SNA levels in China. The GEOS-Chem model and observation data used in this work are described in Sect. 2. The simulation results are evaluated with observations in Sect. 3. In Sect. 4, we will analyze the spatial and temporal distribution of SNA and their relationships to precursor emissions. The concentration changes of SNA in response to the 2000–2015 emission changes are discussed in Sect. 5. The concluding remarks are presented in Sect. 6.

2 Model and observation

2.1 Model and simulations

GEOS-Chem is a global 3-D chemical transport model driven by assimilated meteorological observations from the Goddard Earth Observing System (GEOS) of the NASA Global Modeling Assimilation Office. In this study we use the nested-grid capability of the GEOS-Chem model version 8-02-01 over East Asia (11° S–55° N, 70° E–150° E; Fig. 3) with a horizontal resolution of 0.5° latitude × 0.667° longitude as developed initially by Wang et al. (2004) and extended to the GEOS-5 meteorology by Chen et al. (2009).

The SNA simulation coupled with gas-phase chemistry was developed originally by Park et al. (2004). The aerosol thermodynamic equilibrium in v8-02-01 uses the MARS-A model (Binkowski and Poselle, 2003) which calculates the gas-aerosol phase partitioning of a H_2SO_4–HNO_3–NH_3–H_2O equilibrium system. The wet deposition scheme, including rainout in cloud and washout below cloud, is described by Liu et al. (2001). Dry deposition is based on the resistance-in-series scheme of Wesely (1990) as implemented by Wang et al. (1998).

The GEIA (Global Emission Inventory Activity) inventory (Benkovitz et al., 1996) is the baseline anthropogenic inventory in the GEOS-Chem global model and the global

ACPD
12, 24243–24285, 2012

anthropogenic ammonia emissions are from Bouwman et al. (1997). Scale factors based on energy statistics and other information are used to obtain the emission inventory for the simulation year, as implemented by van Donkelaar et al. (2008) following on the work of Bey et al. (2001) and Park et al. (2004). The GEIA inventory is overwritten by regional emission inventories when available. For East Asia, anthropogenic emissions of NO_x and SO_2 are taken from the inventory of Zhang et al. (2009) for 2006 and NH_3 emissions are taken from Streets et al. (2003) for 2000.

We conducted five series of 15-month simulations with different emissions but the same meteorology from October 2006 to December 2007, with the first 3 months for initialization and the next 12 months for analysis. The simulations are summarized in Table 1. The emission scenarios were formulated on the basis of SO_2 emissions that have long been the primary target of air pollution control policy in China since the 11th FYP. We choose year 2000 to represent the past condition when SO_2 emissions were lowest since 1996 (Lu et al., 2011), 2006 to represent the present case when SO_2 emissions peaked, and 2015 to represent the future scenario, assuming a successful implementation of the 12th FYP to control SO_2. In the 2000 case simulation (2000C), anthropogenic emissions, including SO_2, NO_x and NH_3, were taken from the 2000 emissions inventory by Streets et al. (2003) for East Asia. In the 2006 case simulation (2006C), we adopted the 2006 anthropogenic emissions inventory for East Asia by Zhang et al. (2009), including NO_x and SO_2 but not NH_3. The 2015 case simulation (2015C) uses the same emissions inventory as 2006C but scales the national total of SO_2 and NO_x emissions from their 2006 levels by factors determined as follows: compared to 2006 levels, the national total emissions in 2010 are 9.2 % lower for SO_2 (Lu et al., 2011) and 29.6 % higher for NO_x (Lamsal et al., 2009). According to the 12th FYP, reductions of 8 % and 10 % were applied to SO_2 and NO_x respectively from their emission levels in 2010 to obtain emissions in 2015. The emissions inventory of NH_3 in 2000 from Streets et al. (2003) is used in both 2006C and 2015C. As the emissions estimate for NH_3 is more uncertain than SO_2 and NO_x (Dong et al., 2010; Huang et al., 2011; Huang et al., 2012; Kim et al., 2006; Streets et al., 2003; Zhang et al., 2010), we

ACPD
12, 24243–24285, 2012

set up two more cases – 2006A and 2015A – to investigate the sensitivity of SNA to various NH_3 emissions. Ammonia emissions in 2006A and 2015A are 30 % lower and 16 % higher than those in 2006C and 2015C, respectively. More detailed discussion of NH_3 emissions will be given in Sect. 3. Monthly variation in emissions was adopted from Zhang et al. (2007) for NO_x, Lu et al. (2011) for SO_2, and Fisher et al. (2011) for NH_3. The monthly variability of emissions is the same for all the simulations.

The spatial distributions of SO_2, NO_x and NH_3 emissions over China in 2006C are presented in Fig. 1. High emissions of the three species were concentrated mainly over three regions: North China (NC, 32–42° N, 110–120° E), South China (SC, 22–32° N, 110–120° E), and the Sichuan Basin (SCB, 27–33° N, 102–110° E). Total emissions from the three regions accounted for more than 2/3 of total SO_2, NO_x and NH_3 emissions in China. Among the three regions, emission intensity was highest in NC. The emission intensity of SO_2 was also large in SCB. On the molecular basis, NH_3 emissions was less than the sum of SO_2 and NO_x emissions, indicating poor NH_3 conditions through China in 2006. Figure 2 shows the seasonal variation of the emissions. Emissions of SO_2 and NO_x were highest in DJF and lowest in JJA, whereas NH_3 emissions were highest in JJA and lowest in DJF. The former pattern was driven by heating demand and industry, and the latter was caused by agriculture practice and temperature. The seasonal variation was much larger for NH_3 than for SO_2 or NO_x.

2.2 Observations

There has been no in situ measurement network of aerosols in China that are publicly accessible (Chan and Yao, 2008). We had access to weekly-mean observations of SNA concentrations at two rural sites in China: the Miyun (MY, 40°29′ N, 116°47′ E) site in Beijing and the Beibei (BB, 29°50′ N, 106°25′ E) site in Chongqing. MY is located at the northern edge of North China Plain, about 100 km northeast from Beijing's urban center. There are no distinct anthropogenic pollution sources within 1 km radius of the site. The sampling time was from Januar to December, 2007. BB is located in the Sichuan Basin in Southwest China. It is 10 km from the Beibei city center (a small city

ACPD
12, 24243–24285, 2012

with a population of 650 000) and there are no distinct anthropogenic pollution sources within 2 km of the site. The sampling time was from Februar 2005 to April 2006. At both sites, the aerosol samples were taken with a low flow sampling instrument that collects $PM_{2.5}$ every week. The chemical composition of $PM_{2.5}$ was analyzed in the laboratory. Previous studies (Yang et al., 2011; He et al., 2012) based on SNA observations from these two sites have revealed the concentration levels and composition characteristics, and they indicated that $PM_{2.5}$ compositions at the two sites can be regarded as representative of regional conditions in North and Southwest China.

We also collected annual mean SNA observations during the 2004–2008 period from published studies (Feng et al., 2007; Hagler et al., 2006; Yang et al., 2005; Yang et al., 2008; Wang et al., 2006; Zhang et al., 2012). For model evaluation purposes, monthly mean observations of SNA concentrations in East Asia were obtained from the Acid Deposition Monitoring Network in East Asia (EANET, http://www.eanet.cc/). Wet deposition fluxes of SNA were also collected from EANET to evaluate the simulated SNA budget. Geographical locations of all the observational sites used in this study are shown in Fig. 3 which depicts the nested-grid East Asian model domain (11° S–55° N, 70° E–150° E). Although many of the EANET sites are located outside of China, they lie within the East Asian model domain and thus provide useful observations to evaluate the model.

3 Model evaluation

The GEOS-Chem simulation of SNA has been evaluated with extensive surface observations in the US (Park et al., 2004, 2006; Pye et al., 2009; Leibensperger et al., 2012a; Zhang et al., 2012) and with aircraft measurements of East Asian outflow in springtime (Park et al., 2004; Heald et al., 2005). The model was found capable of reproducing the spatial and seasonal patterns of total SNA and its components. The model generally had small biases in simulating sulfate concentrations and deposition, but tended to overestimate nitrate at the surface. Our model evaluation with observations will focus

ACPD
12, 24243–24285, 2012

on the spatial and seasonal distribution of total SNA (TSNA) and all three components (sulfate, nitrate and ammonium) at the surface over China and East Asia, using simulation results from 2006C.

Figure 4 presents simulated annual-mean distribution of sulfate, nitrate, ammonium, and TSNA at the surface over China, overlaid with surface observations at a few sites. The model has excellent ability in reproducing the observed spatial heterogeneity of TSNA and all three components across China, with high concentrations over NC for all species, over SCB for sulfate and ammonium, and over SC for sulfate. SNA concentrations are lowest in the west, where annual mean TSNA is less than $10\,\mu g\,m^{-3}$. The model has relatively small biases in simulating sulfate, ammonia and TSNA across China, but overestimates nitrate in East China. As indicated before, nitrate overestimation is a common problem found in previous GEOS-Chem studies (Park et al., 2004; Leibensperger et al., 2012; Zhang et al., 2012) as well as in other chemical transport models (Fountoukis et al., 2011; Kim et al., 2006). The reasons are partly attributed to the difficulties in precisely measuring nitrate and partly to the model's treatment of deposition and uncertainties of ammonia emission inventory to be discussed below.

The scatter plot of simulated versus observed seasonal-mean sulfate, nitrate, ammonium and TSNA concentrations at 22 sites in East Asia (20 from EANET, plus MY and BB) are displayed in Fig. 5, with the regression slope and square of correlation coefficient (R^2) given in insert. The model represents a good performance on sulfate simulation with relatively high R^2 ($0.64 \sim 0.79$ by season) and small biases, ranging from −18 % (MAM) to 7 % (SON). The annual mean model bias of sulfate was −10 %. The model had large positive biases (+31 % annually) and poorer correlation for nitrate, with the annual mean R^2 of 0.42 and seasonal-mean R^2 ranging from 0.22 (MAM) to 0.69 (JJA). For ammonium, the model had an annual-mean bias of 35 % and the largest overestimation occurred in JJA (43 %). Despite the bias, the model reproduced the variability of ammonium observation (R^2 = 0.73 annually and 0.57–0.83 by season) well. For the composite TSNA, the model successfully captured the spatial variability (R^2 = 0.58–0.78) and concentration levels of observations with an annual mean bias

ACPD
12, 24243–24285, 2012

of 6 %. This is because the underestimation of sulfate and overestimation of nitrate cancel out in TSNA. As sulfate is the largest component of TSNA in China, the better simulation of sulfate dominates in the comparison for TSNA.

The month to month variation of simulated and observed concentrations of SNA at the MY and BB site is displayed in Fig. 6. At MY, sulfate peaked in JJA, while nitrate and ammonium exhibited double peaks in JJA and DJF. Simulated sulfate levels at MY corresponded well with observations in terms of both variability and concentrations. The model captured the seasonal patterns of observed nitrate and ammonium at MY, but overestimated their concentrations throughout the year by an average of 177 % and 78 %, respectively. The model's bias for nitrate was largest in JJA. At BB, sulfate, nitrate and ammonium all showed a winter maximum and summer minimum. The model reproduced the seasonal variability of observations at BB, with mean biases of −12 %, 46 % and 28 % for sulfate, nitrate and ammonium, respectively.

Wet deposition is the main removal pathway of SNA aerosols from the atmosphere. To evaluate the model's ability of simulating wet deposition, we compared the simulated and observed wet deposition fluxes of SNA at 25 EANET sites (Fig. 7), including 5 Chinese sites and 20 sites in other East Asian countries around China. We found that the model had relatively poor ability in capturing the observed variation of SNA wet deposition (R^2 = 0.18–0.4). The model underestimated wet deposition of sulfate and nitrate by more than 40 %, but the model bias for ammonium wet deposition was not significant. The model's underestimation of nitrate deposition may be one explanation for the model's large overestimation of nitrate concentrations.

As shown above, the major model discrepancy was significant overestimation of nitrate concentrations in China. This is similar to previous studies using GEOS-Chem model (Park et al., 2004 and 2006; Leibensperger et al., 2012; Zhang et al., 2012) and other models such as CMAQ (Kim et al., 2006) and PMCAMx (Fountoukis et al., 2011). The model's underestimation of nitrate wet deposition can partly explain the overestimation of nitrate. In addition, the model overestimated ammonium surface concentrations, indicating that there may be an overestimation of ammonia emissions in

ACPD
12, 24243–24285, 2012

the model. Overestimation of NH_3 favors partitioning of nitrate in the aerosol phase, as ammonium nitrate's formation requires free NH_3 that has not reacted with sulfuric acid. Estimates of NH_3 emissions in China vary greatly among published papers (Streets et al., 2003; Kim et al., 2006; Dong et al., 2010; Zhang et al., 2010; Huang et al., 2011; Huang et al., 2012), suggesting that NH_3 emissions inventories are subject to large uncertainties in China. The most recent estimate of NH_3 emissions in China by Huang et al. (2012) is 9.8 Tg for year 2006, which is much lower than that of 13.5 Tg for 2000 from Streets et al. (2003) and 16.07 Tg for 2006 from Dong et al. (2010). Kim et al. (2006) suggested that the ACE-ASIA NH_3 emissions (Streets et al., 2003) used in their model should be reduced by 20–75 % in order to adjust for the overestimation of nitrate over East Asia. To evaluate the sensitivity of nitrate simulation to NH_3 emissions in the model, we set up the 2006A case, in which NH_3 emissions were reduced by 30 % compared to 2006C. Simulated nitrate and TSNA concentrations were reduced by more than 30 % and 10 % in 2006A, respectively, compared to 2006C, matching better with observations. As expected, there was little change on sulfate concentrations. This suggests that the overestimation of NH_3 emissions in China was the primary reason for nitrate overestimation in the model. Considering the model biases in nitrate and ammonium and the fact that the emission inventory of NH_3 by Streets et al. (2003) for year 2000 was already 38 % too high compared to the latest estimate by Huang et al. (2012) for year 2006, we chose to use the NH_3 inventory for year 2000 from Streets et al. (2003) in 2006C and 2015C, without applying additional increasing factors by year.

Figure 8 shows the observed and simulated (2006C and 2006A) annual mean SNA compositions at the MY and BB sites where we had bi-weekly continuous observations. As discussed before, MY can be regarded as representative of NC and BB as representative of SCB. Observed annual-mean sulfate concentrations were 190 % higher at BB than at MY, which largely contributed to the overall higher TSNA levels at BB than MY. Nitrate concentrations were 10 % higher at BB than at MY. The fractional contribution of sulfate and nitrate to TSNA was 50 % and 26 % at MY, respectively, compared

ACPD
12, 24243–24285, 2012

to that of 66 % and 14 % at BB. The model (both 2006C and 2006A) successfully captured the concentration gradient of TSNA and its components between MY and BB. The 2006C case overestimated the absolute concentrations of nitrate and ammonium and their fractional shares in TSNA at both sites. The overestimation was especially serious for nitrate at MY. In the 2006A case with reduced NH_3 emissions, the model results were much closer to observations.

In summary, the model has good accuracy in simulating the spatial and seasonal distribution of TSNA and its components over China, and has small biases in reproducing surface concentrations of sulfate and TSNA. The overestimation of nitrate was mainly caused by the fact that the currently available bottom-up inventory used in the model overestimated ammonia emissions in China over the 2000–2006 period. Given the model's ability, the following analysis will mainly focus on the changes of TSNA and sulfate in response to precursor emissions changes from 2000 to 2015. We will also examine the changes in nitrate and ammonium from 2000 to 2015, but more in the relative sense, and will involve the NH_3 sensitivity cases (2006A and 2015A).

4 Spatial and seasonal patterns of SNA across China

Since the model can accurately capture the spatial distributions and seasonal patterns of SNA aerosols, we used the model to examine the key factors determining the spatial and seasonal variations of SNA aerosols over China in the present-day case (2006C). This analysis form the basis of understanding the past and future changes of SNA presented in the next section.

Figure 9 shows the seasonal-mean concentrations of TSNA, sulfate, nitrate and ammonium across China. Sulfate is the largest component in total SNA all over China. All SNA species are highest in DJF, followed by SON, and lowest in MAM or JJA. This seasonal pattern was in accordance with that of SO_2 and NO_x emissions. Higher concentrations were distributed over NC, SC and SCB in all seasons, coinciding with the

ACPD
12, 24243–24285, 2012

spatial pattern of highest precursor emissions. Sulfate concentrations were highest in SCB, while nitrate, ammonium, and TSNA were highest in NC.

Figure 10 compares the mean seasonal variations of sulfate, nitrate, ammonium and TSNA averaged over NC, SC and SCB from the 2006C and 2006A cases. As sulfate concentrations showed little sensitivity to the 30 % reduction of NH_3 emissions in 2006A, the 2006A simulation for sulfate is not shown. Sulfate showed a JJA maximum and MAM minimum in NC, whereas an opposite seasonal pattern was found in SC and SCB with a JJA minimum and DJF maximum. The annual mean concentration of sulfate is more or less the same between NC and SC, and it is highest over SCB, reaching about 14 $\mu g\,m^{-3}$. Sulfate made up about 40 % of total SNA mass over NC, and the ratio was highest in JJA (45 %) and lowest in DJF (30 %). By contrast, sulfate contributed 50 % and 60 % to total SNA mass in SC and SCB, respectively, and its fraction in TSNA changed little with seasons in both regions. Both gas- and aqueous-phase oxidation of SO_2 were expected to peak in JJA because of higher temperature, more abundant sunlight, and higher humidity (Yao et al., 2002; Ye et al., 2002; Wang et al., 2006; Zhang et al., 2012). The seasonal pattern of sulfate over NC corresponds with that of oxidation, suggesting that the limiting factor determining the seasonality of sulfate over NC is chemical formation rate of sulfate rather than SO_2 emissions or wet deposition, both of which favor a JJA minimum in sulfate. This is also supported by the fact that annual-mean sulfate concentrations are similar between NC and SC, despite much higher emissions of SO_2 over the former, particularly in winter. Over SC and SCB, the seasonal variation of meteorological factors determining the formation rate of sulfate (i.e., temperature, relative humidity, and solar radiation) is not as pronounced as in NC because of lower latitude. As a result, the seasonality of sulfate over these regions (a DJF maximum and JJA minimum) is driven more by that of SO_2 emissions and wet deposition.

Nitrate shows a DJF maximum over the three regions, which can be explained in part by higher NO_x emissions in winter. As atmospheric NH_4NO_3 formation is constrained strongly by temperature (Wang et al., 2006), the low temperature in winter is favorable

ACPD
12, 24243–24285, 2012

for NH_4NO_3 formation. Nitrate is lowest in spring over NC and in summer over SC and SCB. Among the three regions, nitrate concentrations are highest over NC throughout the year, as both NO_x and NH_3 emissions are highest over this region. Ammonium and TSNA have peak twice over NC, one in winter due to highest nitrate concentrations and one in summer due to highest sulfate concentrations. Over SC and SCB, they are highest in DJF and lowest in JJA, similar to the seasonality of sulfate and nitrate. All SNA species are lowest in spring over NC. High dust loadings over NC in spring can lead to low NO_3^- and SO_4^{2-} (Zhang and Carmichael, 1999; Yao et al., 2002; Fairlie et al., 2010; Zhang et al., 2012). Over SC and SCB, all SNA species are lowest in summer as precipitation, and hence wet scavenging, peak in summer.

We have shown that the mass concentration and composition of SNA aerosols differ by season and region as a result of the temporal and spatial variability in precursor emissions, oxidation rate, and deposition. In the present-day case (2006C), sulfate is the dominant component of SNA over SC and SCB, while nitrate makes an equally important contribution as sulfate over NC. Chemical oxidation rate is the dominant factor in determining SNA concentration levels and seasonality over NC, whereas the key factors are emissions and wet deposition over SC and SCB. Given the regional differences presented above, it is expected that future SNA concentrations over SC and SCB may be more sensitive to SO_2 emission changes, while those over NC may show more complex responses to precursor emissions.

5 SNA variations from 2000 to 2015 due to precursor emission changes

From 2000 to 2006, SO_2 and NO_x emissions in China increased by more than 60 % and 80 % respectively. Since 2006, China has moved aggressively to reduce SO_2 emissions. In the 11th FYP (2006–2010), China set a goal to reduce 10 % of SO_2 emissions in order to control acid rain and PM pollution. It is suggested that this goal was realized and Chinese SO_2 emissions decreased by 9.2 % from 2006 to 2010 (Lu et al., 2011). Zhao et al. (2008, 2010) suggested that the benefits of reducing soil acidification

ACPD
12, 24243–24285, 2012

from SO_2 emission control may be negated by increases of NO_x and NH_3 emissions. NO_x emission reductions were proposed later in the 12th FYP (2011–2015). As elaborated before, we calculated that SO_2 emissions in 2015 will be lower by 16 % and NO_x emissions higher by 16 % compared to the corresponding 2006 levels. Given the large uncertainty in current estimates of NH_3 emissions, we first examined the changes in atmospheric SNA concentrations over China driven by SO_2 and NO_x emissions changes from 2000 to 2015. We then discuss the sensitivity of the future SNA changes to changing NH_3 emissions.

5.1 SNA changes from 2000 to 2006

Figure 11 shows the relative increase of SO_2 and NO_x emissions from 2000 to 2006 over China. There was significant spatial heterogeneity in the emission change patterns across China. Total SO_2 emissions over NC, SC, and SCB in 2006 were 44 %, 87 %, 130 % higher compared with their levels in 2000. Driven by the rapid growth of motor vehicle population, NO_x emissions increased at a faster rate than SO_2 emissions. Total NO_x emissions over the three regions in 2006 were more than twice of those in 2000, with SCB experiencing the largest relative increase (140 %). The emission changes over northwest and northeast China, although large in the relative term, were much smaller in magnitude compared with those in other regions.

Figure 12a shows the absolute difference in annual-mean mass concentrations of sulfate, nitrate, and TSNA between 2006C and 2000C simulations, reflecting the effects of SO_2 and NO_x emission changes from 2000 to 2006 over all regions of China. The concentration change (2006C minus 2000C) was positive over all regions of China, with significant increases distributed in the east, particularly over NC, SC and SCB. The sulfate increase was largest in SCB, by more than 6 $\mu g\,m^{-3}$, compared with that of 4 $\mu g\,m^{-3}$ in NC and SC. The relative increase of sulfate in NC, SC and SCB were 49 %, 64 % and 86 % from 2000 to 2006, corresponding almost linearly to the relative increase of SO_2 emissions in these regions. The nitrate increase was largest in NC, by about 4 $\mu g\,m^{-3}$, compared with that of $1 \sim 2\,\mu g\,m^{-3}$ in SC and SCB. The relative

ACPD
12, 24243–24285, 2012

increase of nitrate, ranging from 40 % to 60 % in the three regions, was much less than the relative increase of NO_x emissions. As NH_3 emissions were held constant from 2000 to 2006 in the simulations, given the large simultaneous increase in SO_2 emissions, there was no excess NH_3 available to form nitrate despite the large increase of NO_x emissions. TSNA concentrations increased by about 10 $\mu g\,m^{-3}$ over the three regions, and the relative change was 54 % ~ 68 % due to the increase of sulfate and nitrate concentrations.

The annual-mean SNA mass concentrations and speciation are summarized by region in Fig. 13. Over NC, nitrate and sulfate made up approximately equal contribution to total mass concentrations of SNA in 2000C and 2006C, and their relative proportions in SNA did not change between the two cases despite increases in their absolute concentrations. This suggests that both SO_2 and NO_x emission changes contributed to increasing SNA concentrations from 2000C to 2006C over NC. Over SC and SCB, however, sulfate was the largest contributor to SNA, making up 45 % and 53 % of mean SNA masses over the two regions in 2000C, respectively. The fractional contribution of sulfate in total SNA increased to 50 % over SC and 60 % over SCB in 2006C, whereas the relative contribution of nitrate in total SNA showed a noticeable decrease from 2000C to 2006C. Over SCB, for example, the fraction of nitrate in TSNA decreased from 21 % in 2000C to 17 % in 2006C, despite a 1.2 $\mu g\,m^{-3}$ increase in nitrate mass concentrations. This suggests that the increase of SO_2 emissions was the main driver of increasing total SNA concentrations over SC and SCB from 2000C to 2006C, with NO_x emission increases playing a secondary role. This is because the formation of $(NH_4)_2SO_4$ is preferential over that of NH_4NO_3 given under constant supply of NH_3 emissions.

5.2 SNA changes from 2006 to 2015

In the 2015C simulation, under the assumption of a successful realization of SO_2 and NO_x emission reduction target during the 12th FYP, total SO_2 and NO_x emissions in China are 16 % lower and 16 % higher than those in 2006C, respectively. The spatial

ACPD
12, 24243–24285, 2012

distribution of NO_x and SO_2 emissions in China is the same between 2006C and 2015C and NH_3 emissions are kept constant.

Figure 12b shows the absolute difference (2015C minus 2006C) in annual-mean mass concentrations of sulfate, nitrate, and TSNA due to SO_2 and NO_x emission changes from 2006 to 2015 over all regions of China. Sulfate decreases all over China, and the largest decrease of sulfate occurs in SCB, reaching up to $7\,\mu g\,m^{-3}$. The average reduction of sulfate over NC, SC, and SCB is $-2\,\mu g\,m^{-3}$ or −14 %, corresponding almost linearly to the −16 % decrease of national total SO_2 emissions from 2006C to 2015C. There is no obvious difference in the relative change of sulfate concentrations between the three regions. By contrast, nitrate shows an increase all over China. The largest absolute increase of nitrate mass concentrations is found over NC, reaching up to $+2\,\mu g\,m^{-3}$ annually. The relative increase of nitrate is much higher over SC and SCB, reaching 23 %. The average mass concentration of nitrate increases by 20 % over China, larger than the +16 % relative increase of national total NO_x emissions between the two cases. This is because the decrease of sulfate in 2015 releases free NH_3 to make additional nitrate. TSNA is found to either decrease or increase depending on the region. Over NC, TSNA mass concentrations increase by 2 %, suggesting that the increase of NO_x emissions outplays the decrease of SO_2 emissions in determining the sign of SNA concentration change. In SCB, TSNA mass concentrations decrease by 5 %, indicating that the effect of SO_2 emission decrease on SNA is larger than that of NO_x emission increase. Over SC, TSNA mass concentrations change little from 2006 to 2015, indicating that the effect of NO_x emission increase balances that of SO_2 emission decrease. Note that the relative change of SO_2 and NO_x emissions from 2006 to 2015 is the same in magnitude although opposite in sign (−16 % for SO_2 and +16 % for NO_x), and such changes are applied uniformly over China without spatial or seasonal differences. Therefore, the different regional change of total SNA in terms of sign and magnitude indicates not only the strong nonlinearity of SNA to precursor emission changes, but also the dependence of such nonlinearity on regional precursor emission mix and composition of SNA.

ACPD
12, 24243–24285, 2012

The chemical composition of SNA aerosols also changes from 2006 to 2015 (Fig. 13). There is a general increase in the proportion of nitrate in total SNA in 2015C compared with 2006C, especially over NC where nitrate's contribution to SNA surpasses that of sulfate and becomes the predominant component of SNA. Over SC and SCB, sulfate is still the largest contributor to total SNA; especially in SCB where sulfate's proportion is greater than 50 %, even in 2015C. The change of concentration levels and speciation of SNA aerosols from 2006C to 2015C suggests that the SO_2 emissions control target set forth by the 12th FYP is effective in reducing total SNA over SC and SCB, but not over NC, for which NO_x emissions control should be strengthened. Furthermore, considering the highest TSNA concentrations, greater efforts should be taken for emissions abatement in this region.

The nonlinear response of SNA to precursor emissions change also differs by season. We summarize the relative change of SNA mass concentrations (2015C minus 2006C) over NC, SC, and SCB in winter (DJF) and summer (JJA) in Table 2. We find that the relative decrease of sulfate in winter is twice that in summer in all three regions despite the same fractional reduction of SO_2 emissions applied in both seasons. As the mass concentration of sulfate peaks in winter except over NC (c.f., Fig. 10), this suggests that SO_2 emissions control is more effective in reducing sulfate levels in winter. The relative change of nitrate mass concentrations is nearly the same in DJF and JJA. Given that mass concentrations of nitrate in winter are typically twice that of those in summer (c.f., Fig. 10), NO_x emissions control should be stressed in winter. Over NC, in which we show above that the increase of NO_x emissions outplays the decrease of SO_2 emissions in determining annual-mean TSNA concentrations, the fractional change of TSNA concentrations is small in magnitude (0.4 ~ 0.5 %) and similar between winter and summer. By contrast, TSNA decreases over SC and SCB and the relative decrease is much higher in winter than in summer.

ACPD
12, 24243–24285, 2012

5.3 Sensitivity of SNA to NH_3 emission change

The discussion in the previous two subsections focuses on the response of SNA over China to past and anticipated future changes of SO_2 and NO_x emissions under the conditions of constant NH_3 emissions from 2006 to 2015. The 2006A case (Sect. 2) examines the impact of the potential high bias in the NH_3 emission inventory for 2006 on simulated present-day SNA concentrations in China. In this subsection, we examine the sensitivity of SNA in 2015 to changes in NH_3 emissions. Dong et al. (2010) suggested that the growth rate of NH_3 emissions in China was stabilized at about 1.5 % per year from 2000 to 2006. As China has not set up any policies to control NH_3 emissions, we assume that NH_3 emissions will increase at this rate from 2006 to 2015. As a result, national total NH_3 emissions will increase by 16 % from 2006 to 2015, which happens to be the same fractional increase as NO_x emissions over this period. This forms a new sensitivity case referred to as 2015A, in which the emissions of NO_x and SO_2 are kept the same as in 2015C.

Figure 12c shows the absolute difference (2015A minus 2006C) in annual-mean mass concentrations of sulfate, nitrate, and TSNA due to the assumed simultaneous changes of SO_2, NO_x, and NH_3 emissions from 2006 to 2015. Sulfate decreases by about 13 % over China in 2015A as compared to 2006C, which is similar to the magnitude of decrease found in 2015C. Although the increase of NH_3 emissions has no influence on sulfate, it results in large enhancement of nitrate, reaching 34–46 % or up to 7 $\mu g\,m^{-3}$ over NC, SC, and SCB. Such an increase is even larger than the linear addition of the fractional increase of both NO_x and NH_3 emissions ($2 \times 16\,\% = 32\,\%$), and this is due to the release of additional free NH_3 to form NH_4NO_3 as a result of decreasing SO_2 emissions. Driven by the large increase of nitrate, TSNA shows an increase all over China. Compared to 2015C, the benefits from SO_2 and NO_x emissions control in stabilizing or reducing SNA are more than offset by the same fractional increase of NH_3 emissions. As shown in Fig. 13, the increase of NH_3 emissions also leads to an increase of nitrate proportion in SNA. Analysis of the 2015A case indicates that NH_3 is

ACPD
12, 24243–24285, 2012

the key factor of determining SNA concentrations in China in the future given the anticipated reduction of SO_2 emissions and increase of NO_x emissions. NH_3 emissions control needs to be enforced along with SO_2 and NO_x emissions control in mitigating SNA concentrations in China in the future.

6 Conclusions

The changes in ground-level mass concentrations and composition of SNA aerosols over China from 2000 to 2015 are simulated using the nested-grid GEOS-Chem model, based on anthropogenic emission changes of SO_2, NO_x, and NH_3 over the past and in the future driven by emissions control target in the 11th and 12th FYP. We show that the model using 2006 emissions has good accuracy in simulating the spatial and seasonal distributions of SNA and its components over China. The model has only small biases in reproducing surface mass concentrations of sulfate and TSNA. Although simulated nitrate and ammonium concentrations correlate well with observations, the model has a large bias of about 30 % for nitrate, which is attributed mainly to the model's overestimation of ammonia emissions in China.

The response of SNA formation to precursor emissions differs by region due to different meteorology and emissions characteristics. The highest concentrations of all SNA species occur over NC, SC, and SCB where the precursor emissions are highest. Chemical oxidation rate is the dominant factor in determining SNA concentration levels and seasonality over NC, whereas the controlling factors are emissions and wet deposition over SC and SCB. In the present-day case (2006), sulfate is the dominant component of SNA over SC and SCB, while nitrate makes an equally important contribution as sulfate over NC.

From 2000 to 2006, SO_2 and NO_x emissions from China increased by 60 % and 82 %, respectively. Total SNA mass concentration increased by about 60 % all over China, most of which was driven by SO_2 emission increase, except over NC where contribution of NO_x emission increase was even larger. From 2006 to 2015, SO_2 and

ACPD
12, 24243–24285, 2012

NO_x emissions from China will change by −16 % and +16 %, respectively, based on the SO_2 and NO_x emissions control target set by the 12th FYP. Under constant NH_3 emissions, sulfate will decrease linearly with SO_2 emission changes, while nitrate will increase more than the percentage increase of NO_x emissions as the decrease of sulfate releases free NH_3 to make NH_4NO_3. TSNA concentrations will either increase or decrease across China, depending on the competition between sulfate reduction and nitrate increase. Over NC, TSNA concentrations will increase by 2 %, experiencing larger impacts from NO_x emission increase, whereas they will decrease by 5 % over SCB with larger effect from SO_2 emissions decrease. Over SC, the two effects cancel out and there will be little change in TSNA concentrations from 2006 to 2015. This analysis suggests that the SO_2 emissions control target set forth by the 12th FYP is effective in reducing SNA over SC and SCB, but not over NC for which NO_x emission control should be strengthened.

We also conducted two sensitivity studies with NH_3 emissions adjusted by −30 % (2006A) and +16 % (2015A) to examine the response of SNA to ammonia emission changes. We found that NH_3 emission changes have no influence on sulfate concentrations, but lead to large changes in nitrate and thus total SNA concentrations. The 2006A simulation reduces the model bias in nitrate and ammonium, suggesting that the currently available bottom-up inventories may overestimate ammonia emissions in China over the 2000–2006 period. Therefore, the future level of NH_3 emissions is uncertain given the lack of sufficient knowledge on the past and present emissions levels of NH_3 in China. If NH_3 emissions are allowed to increase by +16 % from 2006 to 2015 (the same percentage increase as NO_x), nitrate will increase by more than 40 %, more than offsetting the benefit of SO_2 emission reductions over all of China. This sensitivity analysis demonstrates the critical role of NH_3 in regulating nitrate. The policy implication is that the effective strategy to control SNA and hence $PM_{2.5}$ pollution over China should be based on improved understanding of current NH_3 emissions in China and put more emphasis on controlling NH_3 emissions in the future.

ACPD
12, 24243–24285, 2012

Our analysis is an attempt to understand the past and perceived-future response of atmospheric SNA aerosols to precursor emissions changes in China, and to give policy implications for emissions control. Given the uncertainties in estimating future precursor emissions in China especially NH_3 emissions and the model's deficiency in simulating wet deposition, our work cannot be taken as predictions of future SNA levels in China. Further work is clearly needed to conduct careful projections of precursor emissions in the future and to improve the model's performance. More observations containing longer term SNA concentration changes are also needed.

Acknowledgement. This research was supported by the International Science & Technology Cooperation Program of China (2010DFA21300). Y. Wang acknowledges additional funding from the National Science Foundation of China (grant No. 41005060). We thank EANET for providing surface measurements.

References

Adams, P. J. and Seinfeld, J. H.: Global concentrations of tropospheric sulfate, nitrate and ammonium aerosol simulated in a general circulation model, J. Geophys. Res., 104, 13791–13823, 1999.

Ansari, A. S. and Pandis, S. N.: Response of inorganic PM to precursor concentrations, Environ. Sci. Technol., 32, 2706–2714, 1998.

Benkovitz, C. M., Scholtz, M. T., Pacyna, J., Tarrasón, L., Dignon, J., Voldner, E. C., Spiro, P. A., Logan, J. A., and Graedel, T. E.: Global gridded inventories of anthropogenic emissions of sulfur and nitrogen, J. Geophys. Res., 101, 29239–29253, doi:10.1029/96JD00126, 1996.

Bey, I., Jacob, D. J., Yantosca, R. M., Logan, J. A., Field, B. D., Fiore, A. M., Li, Q., Liu, H. Y., Mickley, L. J., and Schultz, M. G.: Global modeling of tropospheric chemistry with assimilated meteorology: model description and evaluation, J. Geophys. Res., 106, 23073–23095, doi:10.1029/2001JD000807, 2001

Binkowski, F. S. and Rpselle, S. J.: Models-3 Community Multiscale Air Quality (CMAQ) model aerosol component, 1, Model description, J. Geophys. Res., 108, 4183, doi:10.1029/2001JD001409, 2003.

ACPD

12, 24243–24285, 2012

Bouwman, A. F., Lee, D. S., Asman, W. A. H., Dentener, F. J., Van der Hoek, K. W., and Olivier, J. G. J.: A global high-resolution emission inventory for ammonia, Global Biogeochem. Cy., 11, 561–587, doi:10.1029/97GB02266, 1997.

Chan, C. K. and Yao, X.: Air pollution in mega cities in China, Atmos. Environ., 42, 1–42, doi:10.1016/j.atmosenv.2007.09.003, 2008.

Chen, D., Wang, Y., McElroy, M. B., He, K., Yantosca, R. M., and Le Sager, P.: Regional CO pollution and export in China simulated by the high-resolution nested-grid GEOS-Chem model, Atmos. Chem. Phys., 9, 3825–3839, doi:10.5194/acp-9-3825-2009, 2009.

Cofala, J., Amann, M., Klimont, Z., Kupiainen, K., and Höglund-Isaksson, L.: Scenarios of global anthropogenic emissions of air pollutants and methane until 2030, Atmos. Environ., 41, 8486–8499, doi:10.1016/j.atmosenv.2007.07.010, 2007.

Dong, W., Xing, J., and Wang, S.: Temporal and spatial distribution of anthropogenic ammonia emissions in China: 1994–2006, Chinese J. Environ. Sci., 31, 1457–1463, 2010 (in Chinese).

EANET: Data report on the acid deposition in the East Asia region 2007, available at: http://www.eanet.cc/product/index.html (last access: July 2012), 2008.

Fairlie, T. D., Jacob, D. J., Dibb, J. E., Alexander, B., Avery, M. A., van Donkelaar, A., and Zhang, L.: Impact of mineral dust on nitrate, sulfate, and ozone in transpacific Asian pollution plumes, Atmos. Chem. Phys., 10, 3999–4012, doi:10.5194/acp-10-3999-2010, 2010.

Fisher, J. A., Jacob, D. J., Wang, Q., Bahreini, R., Carouge, C. C., Cubison, M. J., Dibb, J. E., Diehl, T., Jimenez, J. L., Leibensperger, E. M., Lu, Z., Meinders, M. B. J., Pye, H. O. T., Quinn, P. K., Sharma, S., Streets, D. G., van Donkelaar, A., and Yantosca, R. M.: Sources, distribution and acidity of sulfate- ammonium aerosol in the Arctic in winter–spring, Atmos. Environ., 45, 7301–7318, 2011.

Feng, J. L., Guo, Z. G., Chan, C. K., and Fang, M.: Properties of organic matter in $PM_{2.5}$ at Changdao Island, China – a rural site in the transport path of the Asian continental outflow, Atmos. Environ., 41, 1924–1935, 2007.

Fountoukis, C., Racherla, P. N., Denier van der Gon, H. A. C., Polymeneas, P., Charalampidis, P. E., Pilinis, C., Wiedensohler, A., Dall'Osto, M., O'Dowd, C., and Pandis, S. N.: Evaluation of a three-dimensional chemical transport model (PMCAMx) in the European domain during the EUCAARI May 2008 campaign, Atmos. Chem. Phys., 11, 10331–10347, doi:10.5194/acp-11-10331-2011, 2011.

Hagler, G. S. W., Bergin, M. H., Salmon, L. G., Yu, J. Z., Wan, E. C. H., Zheng, M., Zeng, L. M., Kiang, C. S., Zhang, Y. H., Lau, A. K. H., and Schauer, J. J.: Source areas and chemical com-

ACPD
12, 24243–24285, 2012

position of fine particulate matter in the Pearl River Delta region of China, Atmos. Environ., 40, 3802–3815, 2006.
Heald, C. L., Jacob, D. J., Park, R. J., Alexander, B., Fairlie, T. D., Yantosca, R. M., and Chu, D. A.: Transpacific transport of Asian anthropogenic aerosols and its impact on surface air quality in the United States, J. Geophys. Res., 111, D14310, doi:10.1029/2005JD006847, 2005.
He, K., Zhao, Q., Ma, Y., Duan, F., Yang, F., Shi, Z., and Chen, G.: Spatial and seasonal variability of $PM_{2.5}$ acidity at two Chinese megacities: insights into the formation of secondary inorganic aerosols, Atmos. Chem. Phys., 12, 1377–1395, doi:10.5194/acp-12-1377-2012, 2012.
Hillamo, R., Allegrini, I., Sparapani, R., and Kerminen, V- M.: Mass size distributions and precursor gas concentrations of major inorganic ions in Antarctic aerosol, Int. J. Environ. An. Ch., 71, 353–372, 1998.
Huang, C., Chen, C. H., Li, L., Cheng, Z., Wang, H. L., Huang, H. Y., Streets, D. G., Wang, Y. J., Zhang, G. F., and Chen, Y. R.: Emission inventory of anthropogenic air pollutants and VOC species in the Yangtze River Delta region, China, Atmos. Chem. Phys., 11, 4105–4120, doi:10.5194/acp-11-4105-2011, 2011.
Huang, X., Song, Y., Li, M., Li, J., Huo, Q., Cai, X., Zhu, T., Hu, M., and Zhang, H.: A high-resolution ammonia emission inventory in China, Global Biogeochem. Cy., 26, GB1030, doi:10.1029/2011GB004161, 2012.
Kim, J. Y., Song, C. H., Ghim, Y. S., Won, J. G., Yoon, S. C., Carmichael, G. R., and Woo, J.-H.: An investigation on NH_3 emissions and particulate NH_4^+–NO_3^- formation in East Asia, Atmos. Environ., 40, 2139–2150, 2006.
Koch, D., Park, J., and Genio, A. D.: Clouds and sulfate are anticorrelated: a new diagnostic for global sulfur models, J. Geophys. Res., 108, 4781, doi:10.1029/2003JD003621, 2003.
Lamsal, L. N., Martin, R. V., Padmanabhan, A., van Donkelaar, A., Zhang, Q., Sioris, C. E., Chance, K., Kurosu, T. P., and Newchurch, M. J.: Application of satellite observations for timely updates to global anthropogenic NO_x emissions inventories, Geophys. Res. Lett., 38, L05810, doi:10.1029/2010GL046476, 2011.
Lee, D. S., Köhler, I., Grobler, E., Rohrer, F., Sausen, R., Gallardo-Klenner, L., Oliver, J. G. J., Dentener, F. J., and Bouwman, A. F.: Estimations of global NO_x emissions and their uncertainties, Atmos. Environ., 31, 1735–1749, 1997.

ACPD
12, 24243–24285, 2012

Leibensperger, E. M., Mickley, L. J., Jacob, D. J., Chen, W.-T., Seinfeld, J. H., Nenes, A., Adams, P. J., Streets, D. G., Kumar, N., and Rind, D.: Climatic effects of 1950–2050 changes in US anthropogenic aerosols – Part 1: Aerosol trends and radiative forcing, Atmos. Chem. Phys., 12, 3333–3348, doi:10.5194/acp-12-3333-2012, 2012a.

Leibensperger, E. M., Mickley, L. J., Jacob, D. J., Chen, W.-T., Seinfeld, J. H., Nenes, A., Adams, P. J., Streets, D. G., Kumar, N., and Rind, D.: Climatic effects of 1950-2050 changes in US anthropogenic aerosols – Part 2: Climate response, Atmos. Chem. Phys., 12, 3349–3362, doi:10.5194/acp-12-3349-2012, 2012b.

Liu, H., Jacob, D. J., Bey, I., and Yantosca, R. M.: Constraints from ^{210}Pb and ^{7}Be on wet deposition and transport in a global three-dimensional chemical tracer model driven by assimilated meteorological fields, J. Geophys. Res., 106, 12109–12128, doi:10.1029/2000JD900839, 2001.

Lu, Z., Zhang, Q., and Streets, D. G.: Sulfur dioxide and primary carbonaceous aerosol emissions in China and India, 1996–2010, Atmos. Chem. Phys., 11, 9839–9864, doi:10.5194/acp-11-9839-2011, 2011.

Meng Z., and Seinfeld, J. H.: On the source of the submicrometer droplet mode of urban and regional aerosols, Aerosol Sci. Tech., 20, 253–265, doi:10.1080/02786829408959681, 1994.

Park, R. J., Jacob, D., J., Field, B. D., Yantosca, R. M., and Chin, M.: Natural transboundary pollution influences on sulfate-nitrate-ammonium aerosols in the United States: implications for policy, J. Geophys. Res., 109, D15204, doi:10.1029/2003JD004473, 2004.

Park, R. J., Jacob, D., J., Kumar, N., and Yantosca, R. M.: Regional visibility statistics in the United States: Natural and transboundary pollution influences, and implications for the Regional Haze Rule, Atmos. Environ., 40, 5405–5423, doi:10.1016/j.atmosenv.2006.04.059, 2006.

Pathak, R. K., Wu, W. S., and Wang, T.: Summertime $PM_{2.5}$ ionic species in four major cities of China: nitrate formation in an ammonia-deficient atmosphere, Atmos. Chem. Phys., 9, 1711–1722, doi:10.5194/acp-9-1711-2009, 2009.

Pinder, R. W. and Adams, P. J.: Ammonium emission controls as a cost-effective strategy for reducing atmospheric particulate matter in the East United States, Environ. Sci. Tchenol., 41, 380–386, 2007.

Pye, H. O., Liao, H., Wu, S., Mickley, L. J., Jacob, D. J., Henze, D. K., and Seinfeld, J. H.: Effect of changes in climate and emissions on future sulfate-nitrate-ammonium aerosol levels in the United States, J. Geophys. Res., 114, D01205, doi:10.1029/2008JD010701, 2009.

ACPD
12, 24243–24285, 2012

Querol, X., Alastuey, A., Ruiz, C. R., Artinano, B., Hansson, H. C., Harrison, R. M., Buringh, E., ten Brink, H. M., Lutz, M., Bruckmann, P., Straehl, P., and Schneider, J.: Speciation and origin of PM_{10} and $PM_{2.5}$ in selected European cities, Atmos. Environ., 38, 6547–6555, 2004.

Seinfeld, J. H. and Pandis, S. N.: Atmospheric Chemistry and Physics: From Air Pollution to Climate Change, John Wiley, Hoboken, NJ, 1998.

Smith, S. J., van Aardenne, J., Klimont, Z., Andres, R. J., Volke, A., and Delgado Arias, S.: Anthropogenic sulfur dioxide emissions: 1850–2005, Atmos. Chem. Phys., 11, 1101–1116, doi:10.5194/acp-11-1101-2011, 2011a.

Smith, S. J., Pitcher, H., and Wigley, T. M. L.: Global and regional anthropogenic sulfur dioxide emissions, Global Planet. Change, 29, 99–119, 2001b.

Streets, D. G., Bond, T. C., Carmichael, G. R., Fernandes, S. D., Fu, Q., He, D., Klimont, Z., Nelson, S. M., Tsai, N. Y., Wang, M. Q., Woo, J.-H., and Yarber, K. F.: An inventory of gaseous andprimary aerosol emissions in Asia in the year 2000, J. Geophys. Res., 108, 8809, doi:10.1029/2002JD003093, 2003.

Tsimpidi, A. P. and Karydis, V. A.: Response of inorganic fine particulate matter to emission changes of sulfur dioxide and ammonia: the easten united states as a case study, J. Air Waste Manage. Assoc., 57, 1489–1498, doi:10.3155/1047-3289.57.12.1489, 2007.

Tsimpidi, A. P. and Karydis, V. A.: Response of fine particulate matter to emission changes of oxidies of nitrogen and anthropogenic volatile organic compounds in the Eastern United States, J. Air Waste Manage. Assoc., 58, 1463–1473, doi:10.3155/1047-3289.58.11.1463, 2008.

Unger, N., Shindell, D. T., Koch, D. M., and Streets, D. G.: Cross influences of ozone and sulfate precursor emissions changes on air quality and climate, P. Natl. Acad. Sci. USA, 103, 4377–4380, 2006.

van Donkelaar, A., Martin, R. V., Leaitch, W. R., Macdonald, A. M., Walker, T. W., Streets, D. G., Zhang, Q., Dunlea, E. J., Jimenez, J. L., Dibb, J. E., Huey, L. G., Weber, R., and Andreae, M. O.: Analysis of aircraft and satellite measurements from the Intercontinental Chemical Transport Experiment (INTEX-B) to quantify long-range transport of East Asian sulfur to Canada, Atmos. Chem. Phys., 8, 2999–3014, doi:10.5194/acp-8-2999-2008, 2008.

Wang, Y., Jacob, D. J., and Logan, J. A.: Global simulation of tropospheric O_3-NO_x-hydrocarbon chemistry, 1, model formulation, J. Geophys. Res., 103, 10713–10726, 1998.

ACPD
12, 24243–24285, 2012

Wang, Y. X., McElroy, M. B., Jacob, D. J., and Yantosca, R. M.: A nested grid formulation for chemical transport over Asia: Applications to CO, J. Geophys. Res., 109, D22307, doi:10.1029/2004JD005237, 2004.

Wang, Y., Zhuang, G., Zhang, X., Huang, K., Xu, C., Tang, A., Chen, J., and An, Z.: The ion chemistry, seasonal cycle, and sources of $PM_{2.5}$ and TSP aerosol in shanghai, Atmos. Environ., 40, 2935–2952, 2006.

Watson, J. G.: Critical review–visibility: science and regulation, J. Air Waste Manage., 52, 628–713, 2002.

Wesely, M. L.: Parameterization of surface resistance to gaseous dry deposition in regional-scale numerical models, Atmos. Environ., 23, 1293–1304, 1989.

Xing, J., Wang, S. X., Chatani, S., Zhang, C. Y., Wei, W., Hao, J. M., Klimont, Z., Cofala, J., and Amann, M.: Projections of air pollutant emissions and its impacts on regional air quality in China in 2020, Atmos. Chem. Phys., 11, 3119–3136, doi:10.5194/acp-11-3119-2011, 2011.

Yang, F., Tan, J., Zhao, Q., Du, Z., He, K., Ma, Y., Duan, F., Chen, G., and Zhao, Q.: Characteristics of $PM_{2.5}$ speciation in representative megacities and across China, Atmos. Chem. Phys., 11, 5207–5219, doi:10.5194/acp-11-5207-2011, 2011.

Yang, H., Yu, J. Z., Ho, S. S. H., Xu, J. H., Wu, W. S., Wan, C. H., Wang, X. D., Wang, X. R., and Wang, L. S.: The chemical composition of inorganic and carbonaceous materials in $PM_{2.5}$ in Nanjing, China, Atmos. Environ., 39, 3735–3749, 2005.

Yang, L.: Characterization and source apportionment of $PM_{2.5}$ andits impact on visibility in Jinan, PhD thesis, Shandong University, Jinan, 2008 (in Chinese).

Yao, X., Chan, C. K., Fang, M., Cadle, S., Chan, T., Mulawa, P., He, K., and Ye, B.: The water-soluble ionic composition of $PM_{2.5}$ in Shanghai and Beijing, China, Atmos. Environ., 36, 4223–4234, 2002.

Ye, B., Ji, X., Yang, H., Yao, X., Chan, C. K., Cadle, S. H., Chan, T., and Mulawa, P. A., Concentration and chemical composition of $PM_{2.5}$ in Shanghai for a 1-year period, Atmos. Environ., 37, 499–510, 2002.

Zhang, L., Jacob, D. J., Knipping, E. M., Kumar, N., Munger, J. W., Carouge, C. C., van Donkelaar, A., Wang, Y. X., and Chen, D.: Nitrogen deposition to the United States: distribution, sources, and processes, Atmos. Chem. Phys., 12, 4539–4554, doi:10.5194/acp-12-4539-2012, 2012.

Zhang, Q., Streets, D. G., He, K., Wang, Y. X., Richter, A., Burrows, J. P., Uno, I., Jang, C. J., Chen, D., Yao, Z., and Lei, Y.: NO_x emission trends for China, 1995–2004:

ACPD
12, 24243–24285, 2012

the view from the ground and the view from space, J. Geophys. Res., 112, D22306, doi:10.1029/2007JD008684, 2007

Zhang, Q., Streets, D. G., Carmichael, G. R., He, K. B., Huo, H., Kannari, A., Klimont, Z., Park, I. S., Reddy, S., Fu, J. S., Chen, D., Duan, L., Lei, Y., Wang, L. T., and Yao, Z. L.: Asian emissions in 2006 for the NASA INTEX-B mission, Atmos. Chem. Phys., 9, 5131–5153, doi:10.5194/acp-9-5131-2009, 2009.

Zhang, X. Y., Wang, Y. Q., Niu, T., Zhang, X. C., Gong, S. L., Zhang, Y. M., and Sun, J. Y.: Atmospheric aerosol compositions in China: spatial/temporal variability, chemical signature, regional haze distribution and comparisons with global aerosols, Atmos. Chem. Phys., 12, 779–799, doi:10.5194/acp-12-779-2012, 2012.

Zhang, Y., and Carmichael, G. R.: The role of mineral aerosol in tropospheric chemistry in East Asia – a model study, J. Appl. Meteorol., 38, 353–366, 1999.

Zhang, Y., Dore, A. J., Ma, L., Liu, X. J., Ma, W. Q., Cape, J. N., and Zhang, F. S.: Agricultural ammonia emissions inventory and spatial distribution in the North China Plain, Environ. Pollut., 158, 490–501, doi:10.1016/j.envpol.2009.08.033, 2010.

Zhao, Y., Wang, S. X., Duan, L., Lei, Y., Cao, P. F., and Hao, J. M.: Primary air pollutant emissions of coal-fired power plants in China: current status and future prediction, Atmos. Environ. 42, 8442–8452, 2008.

Zhao, Y., Duan, L., Lei, Y., Xing, J., Nielsen, C. P., and Hao, J.: Will PM control undermine China's efforts to reduce soil acidification?, Environ. Pollut., 159, 2726–2732, 2011.

ACPD
12, 24243–24285, 2012

Table 1. Simulation description.

Simulation name	Emission Year	SO_2 emissions (Tg)	NO_x emissions (Tg)	NH_3 emissions (Tg)	Year of meteorology
2006C	2006	31	20.8	13.5	2007
2000C	2000	19.3	11.4	13.5	2007
2015C	2015	25.9	24.26	13.5	2007
2006A	2006	31	20.8	9.45	2007
2015A	2015	25.9	24.26	15.73	2007

ACPD
12, 24243–24285, 2012

Table 2. The percentage change of sulfate, nitrate and TSNA mass concentrations from 2006C to 2015C (2015C minus 2006C), averaged for summer (June, July, August; JJA) and winter (December, January, February; DJF).

		sulfate	nitrate	TSNA
NC	DJF	−19 %	17 %	0.5 %
	JJA	−10 %	19 %	0.4 %
SC	DJF	−19 %	29 %	−2 %
	JJA	−11 %	21 %	0.2 %
SCB	DJF	−19 %	20 %	−7 %
	JJA	−10 %	20 %	−4.5 %

ACPD
12, 24243–24285, 2012

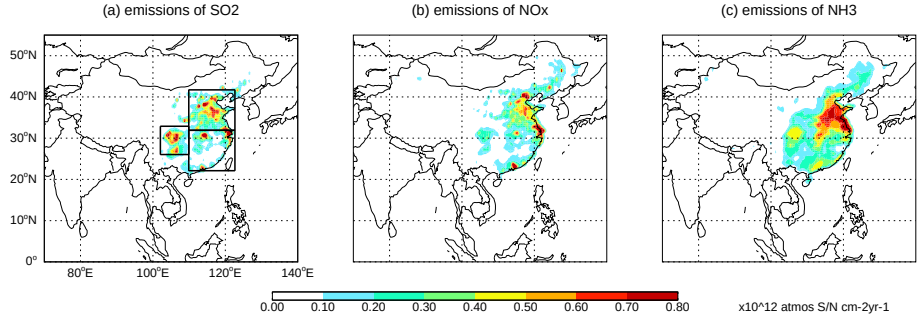

Fig. 1. Spatial distributions of **(a)** SO_2, **(b)** NO_x and **(c)** NH_3 emissions from China used in 2006C simulation.

ACPD
12, 24243–24285, 2012

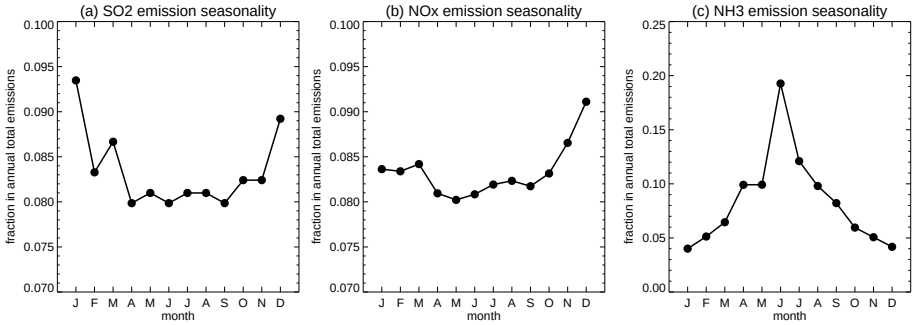

Fig. 2. Seasonality of **(a)** SO_2, **(b)** NO_x and **(c)** NH_3 emissions from China.

ACPD
12, 24243–24285, 2012

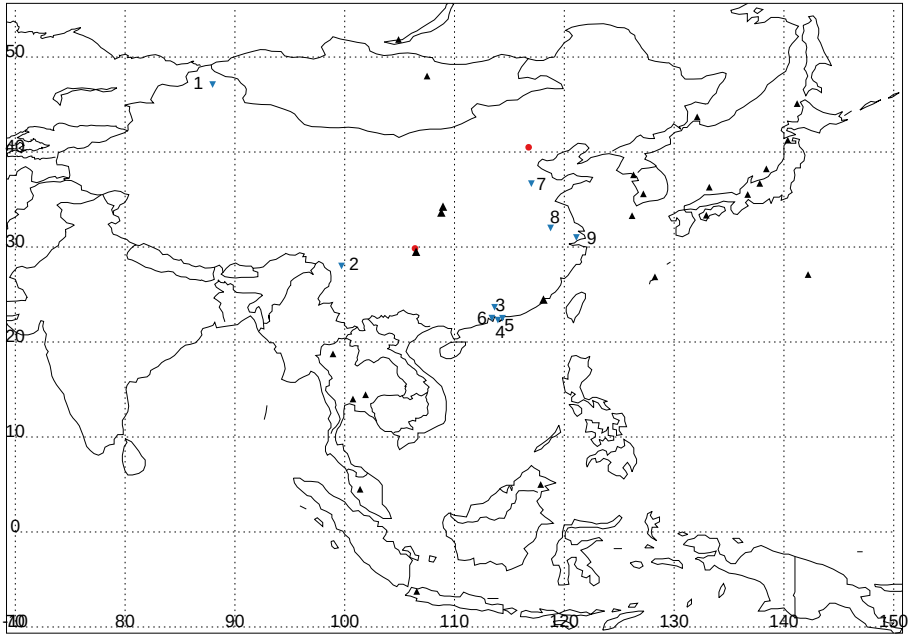

Fig. 3. Locations of observational data used in this study. The black triangles represent 25 sites from EANET; the red circles represent Miyun and Beibei sites with weekly observations; blue inverted triangles represent 10 Chinese rural sites from published papers: (1) Akdala, (2) Shangrl-La (Zhang et al., 2012); (3) Conghua, (4) Tung Chung, (5) Tap Yun, (6) Zhongshan (Hagler et al., 2006); (7) Jinan (Yang, 2008); (8) Nanjing (Yang et al., 2005), and (9) Shanghai (Wang et al., 2006).

ACPD
12, 24243–24285, 2012

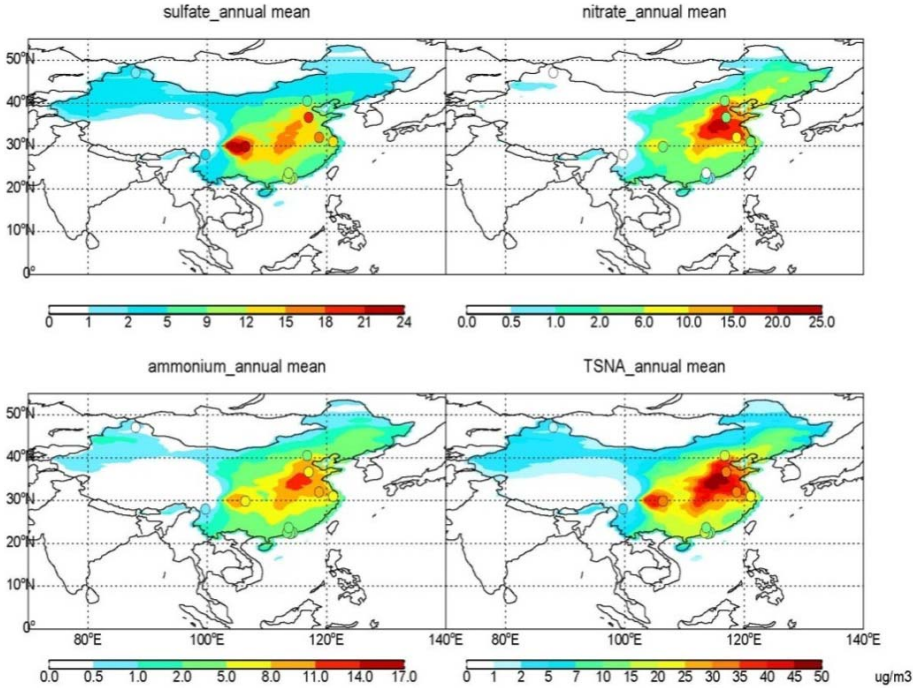

Fig. 4. Overlay of simulated (color map) and observed (colored circles) annual mean surface concentrations of total SNA (TSNA), sulfate, nitrate and ammonium over China. Observations are derived from the MM and BB sites with weekly measurements and from the 10 sites in published literatures (i.e., the blue triangle sites shown in Fig. 3).

ACPD
12, 24243–24285, 2012

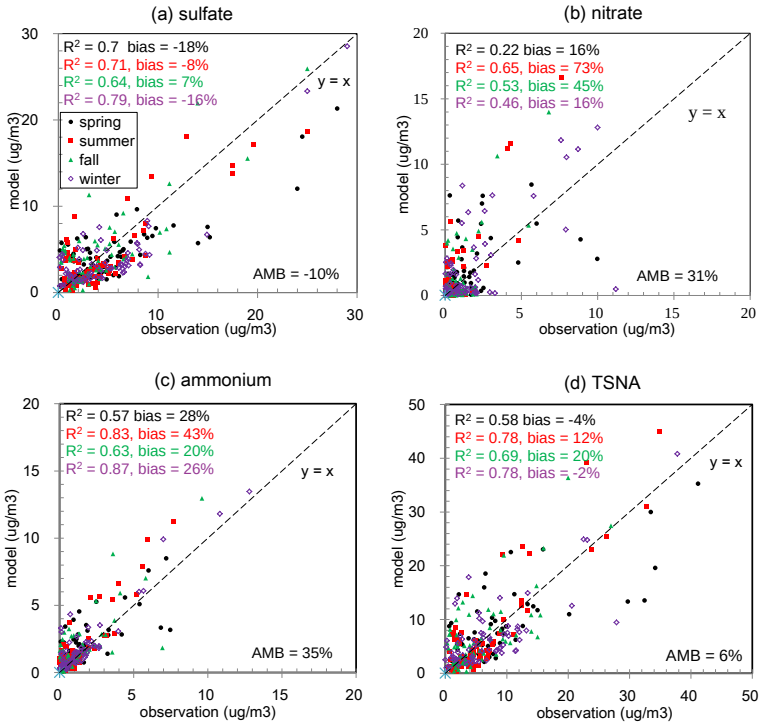

Fig. 5. Scatter plots of simulated versus observed SNA concentrations at 23 (the 4 EANET sites inside China have no observation data for SNA) sites in East Asia, including 2 sites in China (BB and MY) and 21 sites from other countries. Values are seasonal mean for 2006. The black dots represent spring, the red squares represent summer, the green triangles represent fall, and the violet hollow diamonds represent winter. AMB = annual mean bias. The square of correlation coefficient (R^2), normalized mean bias, and annual mean bias (AMB) are given in the figure. The $y = x$ relationship (dashed lines) is shown.

ACPD
12, 24243–24285, 2012

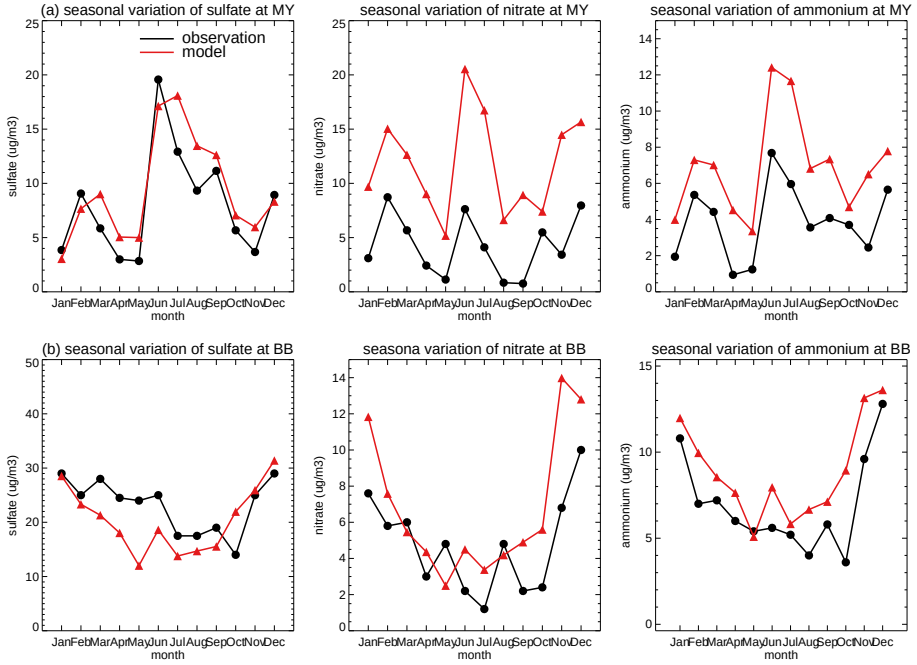

Fig. 6. The month to month variations of simulated and observed mass concentrations of sulfate, nitrate and ammonium (left to right) at the **(a)** MY and **(b)** BB site. The black lines represent observations and the red lines represent the simulation.

ACPD
12, 24243–24285, 2012

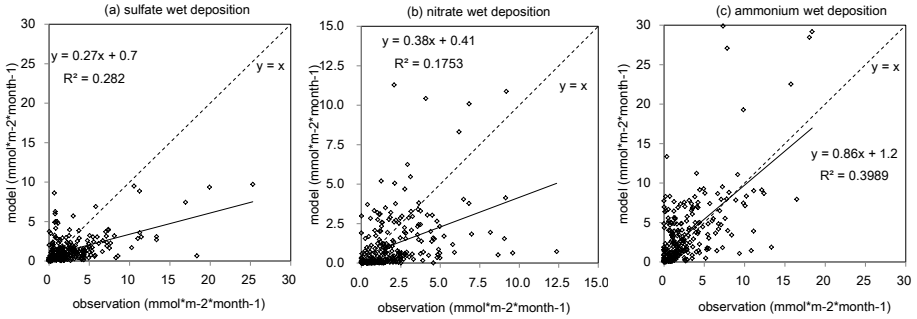

Fig. 7. Scatter plots of simulated (y-axis) versus observed (x-axis) SNA wet deposition fluxes. The square of correlation coefficient (R^2) and the normalized mean bias are given.

ACPD
12, 24243–24285, 2012

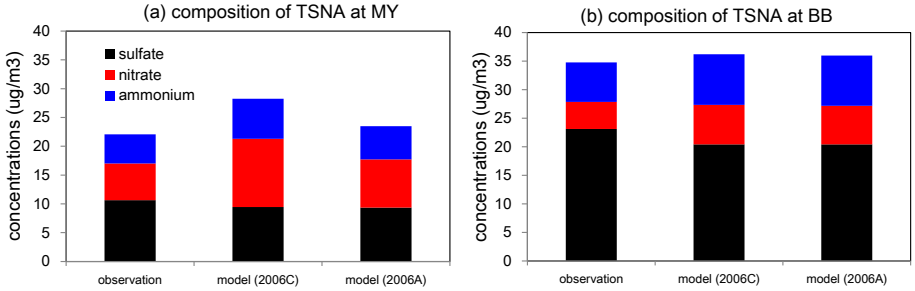

Fig. 8. Observed and simulated annual-mean SNA composition and concentrations at the **(a)** MY and **(b)** BB site. Model results from 2006C and 2006A simulations are displayed.

ACPD
12, 24243–24285, 2012

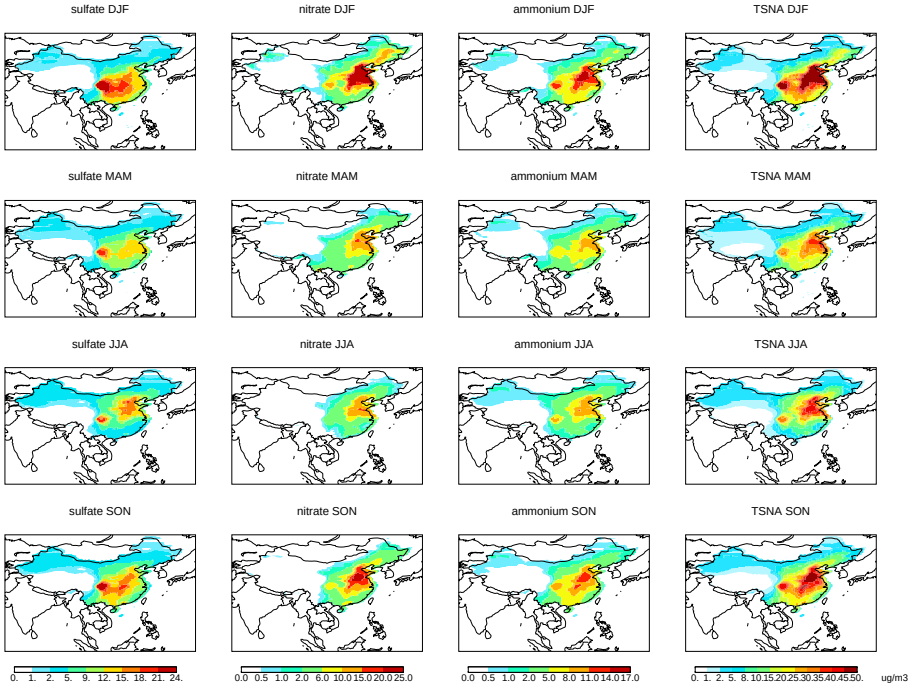

Fig. 9. Simulated seasonal-mean surface concentrations of sulfate, nitrate, ammonium and TSNA (left to right) in December–February (DJF), March–May (MAM), June–August (JJA) and September–November (SON), 2006.

ACPD
12, 24243–24285, 2012

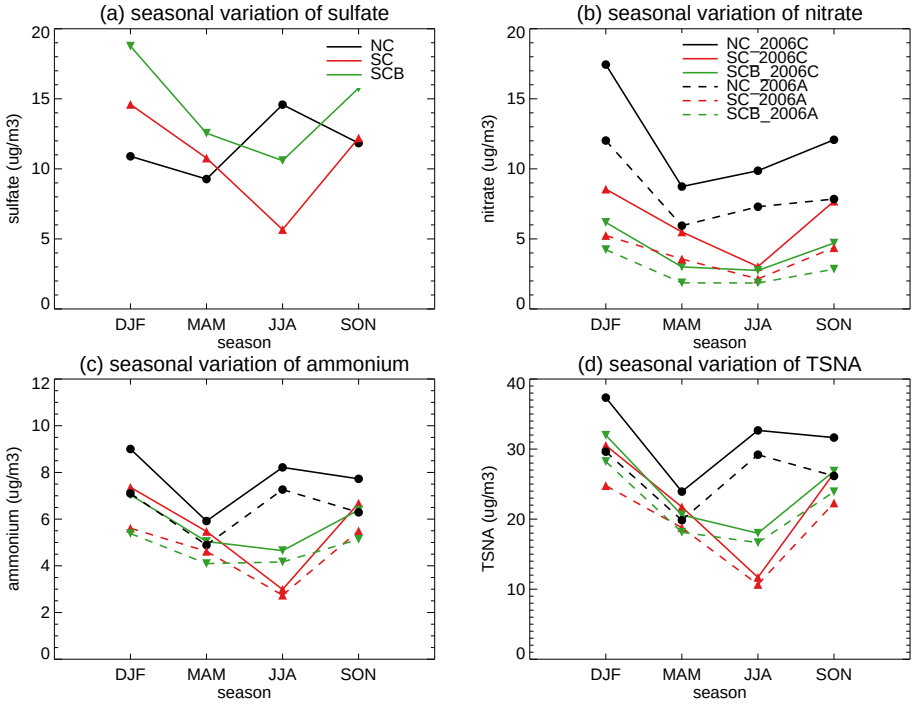

Fig. 10. Simulated seasonal mean concentrations of **(a)** sulfate, **(b)** nitrate, **(c)** ammonium and **(d)** TSNA over NC, SC and SCB. The black lines represent NC, red lines represent SC and blue lines represent SCB. The solid lines represent 2006C results and dashed lines represent 2006A results.

ACPD
12, 24243–24285, 2012

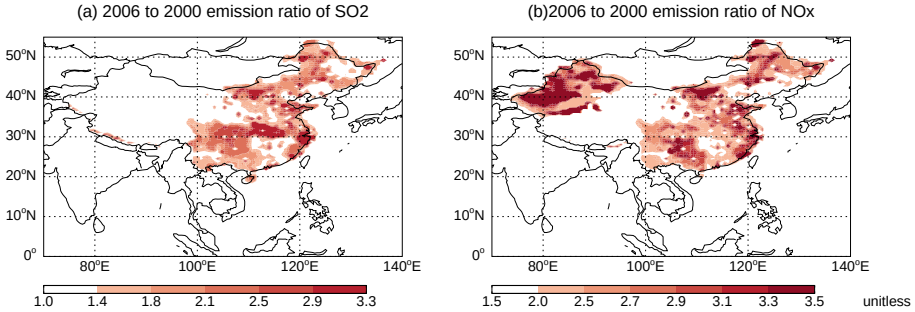

Fig. 11. SO_2 and NO_x emission changes from 2000 to 2006 in China. The data shown are the ratio of 2006 emissions to 2000 emissions.

ACPD
12, 24243–24285, 2012

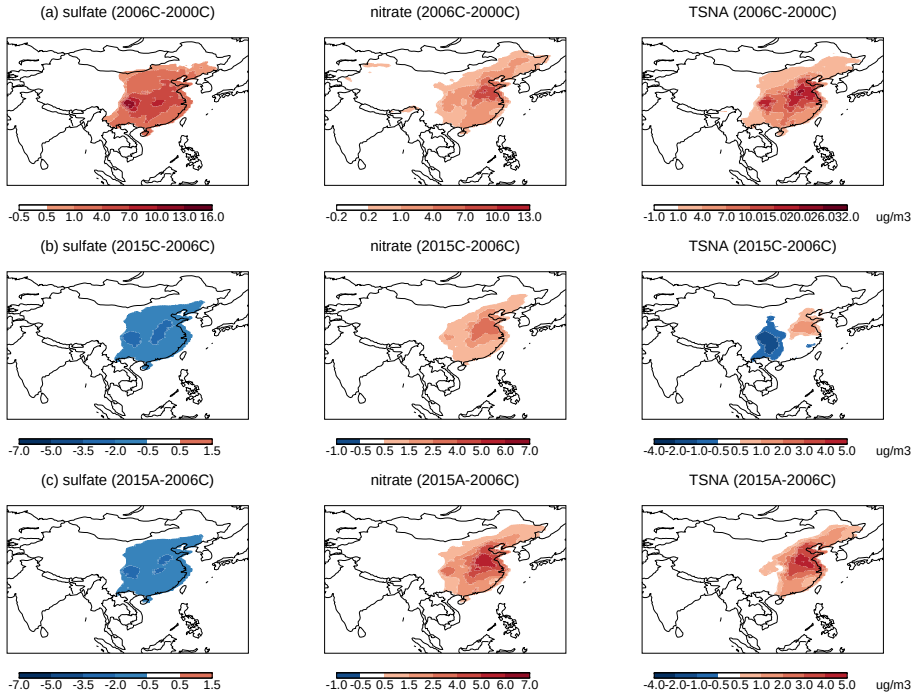

Fig. 12. The changes in mass concentrations of sulfate (left), nitrate (middle), and TSNA (right) from 2000 to 2015. **(a)** the changes from 2000C to 2006C; **(b)** the changes from 2006C to 2015C; **(c)** the changes from 2006C to 2015A. Note that the color scale in **(a)** is different from that in **(b)** or **(c)**.

ACPD
12, 24243–24285, 2012

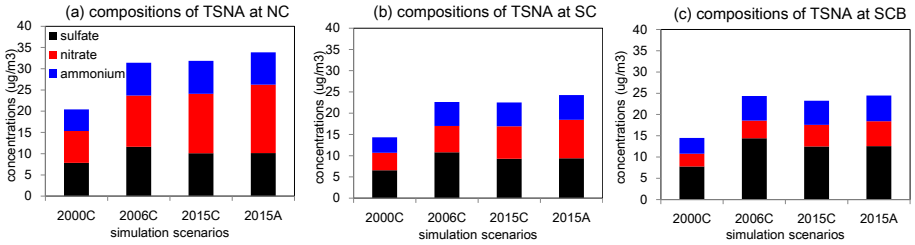

Fig. 13. Simulated composition and concentration changes of SNA aerosols from 2000 to 2015 over **(a)** NC, **(b)** SC and **(c)** SCB. Four simulation cases are compared: 2000C, 2006C, 2015C, and 2015A.

ACPD
12, 24243–24285, 2012